Structure determination of individual single-wall carbon nanotubes by nanoarea electron diffraction

M. Gao, J. M. Zuo,[a] R. D. Twesten, and I. Petrov
Department of Materials Science and Engineering and Materials Research Laboratory, University of Illinois at Urbana-Champaign, Illinois 61801

L. A. Nagahara and R. Zhang
Physical Sciences Research Laboratories, Motorola Labs, 7700 South River Parkway, Tempe Arizona 85284

(Received 13 December 2002; accepted 21 February 2003)

In this letter, we report an electron diffraction determination of chiral vectors (n,m) of individual single-wall carbon nanotubes (SWNTs). Electron diffraction patterns from individual SWNTs were recorded on imaging plates using a parallel electron beam over a section of tube of ~50 nm long. Using two tubes of 1.39 and 3.77 nm in diameter, we show that the details of electron diffuse scattering can be detected for both the small and large tubes. The quality of diffraction patterns allows the accurate measurement of both the diameters and chiral angles of SWNTs for a direct determination of chiral vectors. The electron diffraction technique is general and applicable to other forms of individual nanostructures. © *2003 American Institute of Physics.*
[DOI: 10.1063/1.1569418]

Carbon nanotubes (CNTs) represent an important type of nanostructure. Since Iijima showed the high-resolution transmission electron microscopy (HRTEM) image and electron diffraction of multiwall CNTs,[1] CNTs have attracted extraordinary attention due to their unique physical properties, from atomic structure to mechanical and electronic properties.[2–4] A single-wall CNT (SWNT) can be regarded as a single layer of graphite that has been rolled up into a cylindrical structure. In general, the tube is helical with the chiral vector (n,m) defined by $\mathbf{c}=n\mathbf{a}+m\mathbf{b}$, where $\mathbf{c}$ is the circumference of the tube, and $\mathbf{a}$ and $\mathbf{b}$ are the unit vectors of the graphite sheet (we use $a=b=2.461$ Å and $\gamma=60°$). A striking feature is tubes with $n-m=3l$ (l is a integer) are metallic, while others are semiconductive.[5,6] This unusual property, plus the apparent stability, has made CNTs an attractive material for constructing nanoscale electronic devices.[7] As-grown SWNTs have a dispersion of chirality and diameters;[3,4] the nanotube structural energy is only weakly dependent on chirality.[8] Hence, a critical issue in CNT applications and science study is the structure determination of a given individual tube.[9] This requires a structural probe that can be applied to individual nanotubes.

The determination of the chiral vector requires the measurement of both diameter and chiral angle. Since Iijima's initial study, many articles has been published on structural characterization using electron diffraction,[1,10–15] scanning tunneling microscopy (STM),[16,17] and Raman spectroscopy.[9] Among these techniques, STM and electron diffraction have the selectivity that can be used to study individual tubes. STM resolves the structure of a part of the outer wall of carbon nanotube to measure the chiral angle, however, STM cannot be used alone to distinguish between different forms of tubes. Electron diffraction in principle can determine unambiguously both the chirality and diameter of tubes. However, with the exception of the recent work on a large double wall tube (6.6 nm),[13] published electron diffraction studies focus on multiwall CNTs or single wall CNT bundles. HRTEM imaging is used widely to measure tube diameters, but its accuracy is a few angstroms, which greatly depends on electron defocus and tube size.[18] Individual SWNTs are very difficult to characterize.[14,15] Previously published diffraction patterns of individual SWNTs are blurred and features are difficult to identify.[10,11] The reason is that electron diffraction from a SWNT can be extremely weak and often beyond the sensitivity of conventional selected area electron diffraction (SAED). Thus, despite the importance, quantitative determination of a SWNT structure by electron diffraction so far has not been done.

Here we report the quantitative structure determination of SWNTs by nanoarea electron diffraction in a field-emission electron microscope and recording with imaging plates. This, coupled with improved electron diffraction pattern interpretation, allows us to determine both the diameter and chiral angle, thus the chiral vector (n,m), from an individual SWNT. The technique developed here is general. When used together with transport measurement this will give an unambiguous determination of the structure-property relationship of SWNTs.[13]

The carbon nanotubes studied here were grown by chemical vapor deposition. Catalyst was prepared following the approach reported by Cassell *et al.*[19] Transmission electron microscopy (TEM) observation was carried out in a JEOL2010F TEM with a high voltage of 200 keV. Diffraction patterns were recorded on imaging plates with the camera length of 80 cm and exposure time 11 s.

Figure 1 shows a schematic diagram of the principle of parallel-beam nanoarea electron diffraction in a TEM. The electron beam is focused to the focal plane of the objective prefield and forms a parallel beam illumination on the sample. The size of the parallel probe is determined by the condenser aperture. For an aperture of 10 μm in diameter,

[a]Author to whom correspondence should be addressed; electronic mail: jianzuo@uiuc.edu

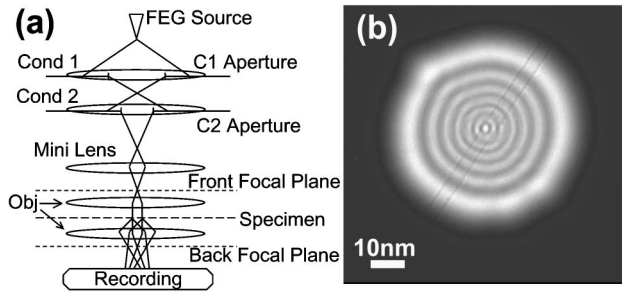

FIG. 1. (a) Schematic ray diagram of nanoarea electron diffraction. A parallel beam is formed by focusing electron onto the front-focal plane of preobjective lens. The beam size is determined by condenser aperture. (b) An image of the electron probe formed by a 10 μm condenser aperture with a large tube illuminated. The probe current intensity is $\sim 10^5$ e/s nm^2 with a Schottky field emission gun.

the probe diameter is ~50 nm, which is much smaller than conventional SAED, and does not suffer from aberration induced image shift.[20] Nanoarea electron diffraction in a FEG microscope also provides higher beam intensity than SAED (the probe current intensity is $\sim 10^5$ e/s nm^2). Both are important for the investigation of CNTs because of the small scattering cross section of carbon and the requirement of a straight tube for electron diffraction. Figure 1(b) shows a real space image of the incident probe on a CNT. The beam damage to the CNT is carefully controlled to a minimum, much less than that of HRTEM imaging.

Figure 2(a) shows the diffraction pattern from a SWNT. The main features of this pattern are as follows: (1) a relatively strong equatorial oscillation which is perpendicular to the tube direction; (2) some very weak diffraction lines from the graphite sheet, which are elongated in the direction normal to the tube direction.[1,15] The intensities of diffraction lines are very weak in this case. In our experimental setup introduced earlier, the strongest intensity of one pixel for $(1\bar{1}00)$ diffraction lines is about 10, which corresponds to ~12 electrons.

We determine both the diameter and chiral angle from the electron diffraction pattern alone. The diameter is determined from the equatorial oscillation, while the chiral angle is determined by measuring the distances from the diffraction lines to the equatorial line. The details are following. The diffraction of SWNT is well described by kinematic diffraction theory. The equatorial oscillation in the Fourier transformation of a helical structure like SWNT is a Bessel function with $n=0$,[21] which gives

$$I_0(X) \propto J_0^2(X) \propto \left| \int_0^{2\pi} \cos^{X \cos \Omega} d\Omega \right|^2. \quad (1)$$

Here $X = 2\pi R r_0 = \pi R D_0$, R is the reciprocal vector which can be measured from the diffraction pattern and D_0 is the diameter of the SWNT. We use the position of $J_0^2(X)$ maxima (X_n, $n=0,1,2,...$) to determine the tube diameter. With the first several maxima saturated and unaccessible, X_n/X_{n-1} can be used to determine the number N for each maximum in the equatorial oscillation. Thus, by comparing the experimental equatorial oscillation with values of X_n, the tube diameter can be uniquely determined.

To measure chirality from the diffraction pattern, Fig. 2(d) is considered, which shows the geometry of the SWNT

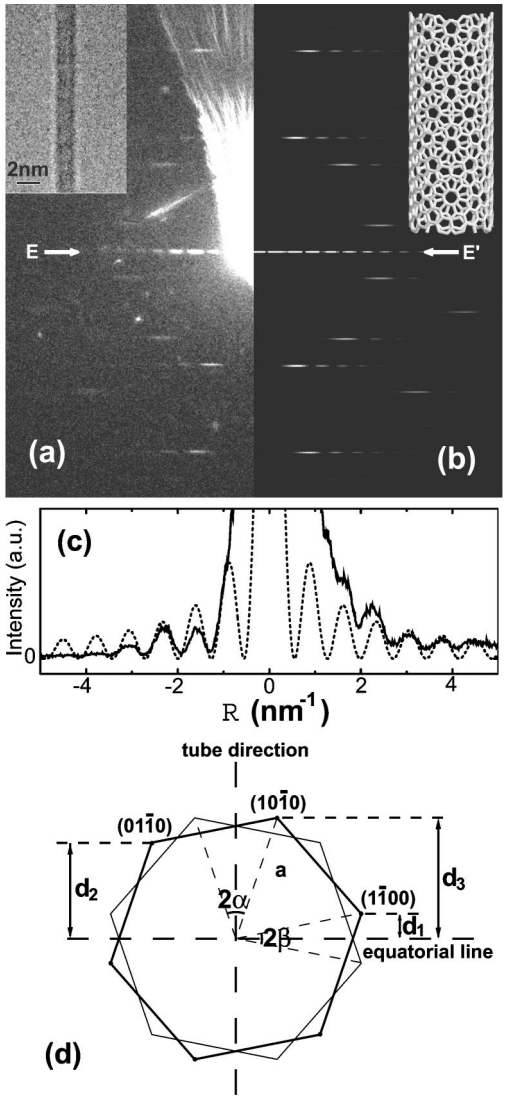

FIG. 2. (a) A diffraction pattern from an individual SWNT of 1.4 nm in diameter. The inset is a TEM image. The radial scattering around the saturated (000) is an artifact from aperture scattering. (b) A simulated diffraction pattern of a (14,6) tube. The inset is the corresponding structure model. (c) Profiles of equatorial oscillation along EE' from Fig. 2(a) and simulation for (14,6). (d) A schematic diagram of electron diffraction from an individual SWNT. The two hexagons represent the first order graphite-like $\{10\bar{1}0\}$ diffraction spots from the top and bottom of the tube.

diffraction pattern based on the diffraction of the top-bottom graphite sheets. The distances d_1, d_2, d_3 relate to the chiral angle α by

$$\alpha = \text{atan}\left(\frac{1}{\sqrt{3}} \cdot \frac{d_2 - d_1}{d_3}\right) = \text{atan}\left(\frac{1}{\sqrt{3}} \cdot \frac{2d_2 - d_3}{d_3}\right). \quad (2)$$

These relationships are not affected by the tilting angle of the tube (see later). Because d_2 and d_3 are corresponding to the diffraction lines having relatively strong intensities and are further from the equatorial line, they are used in our study instead of d_1 to reduce the error. The distances can be measured precisely from the digitalized patterns. The errors are estimated to be $<1\%$ for the diameter determination and $<0.2°$ for the chiral angle.

Using the earlier methods, the SWNT giving diffraction pattern shown in Fig. 2(a) was determined to have a diameter of 1.40 nm (± 0.02 nm) and a chiral angle of 16.9° ($\pm 0.2°$).

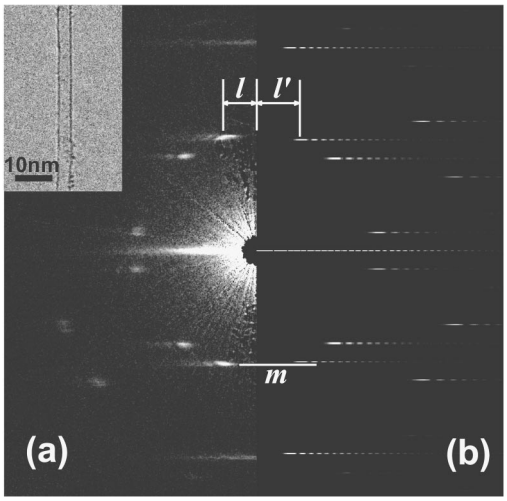

FIG. 3. (a) A diffraction pattern from a tube of 3.77 nm in diameter. The inset is a TEM image. (b) A simulated diffraction pattern of a (35,20) tube. The tube was inclined at an angle of 77° to the electron beam. Line "*m*" is the extension of $(10\bar{1}0)$ diffraction line in the experimental pattern, which is further than that of simulation.

Among the possible chiral vectors, the best match is (14,6), which has a diameter and chiral angle of 1.39 nm and 17.0°, respectively. The closest alternative is (15,6), having a diameter of 1.47 nm and chiral angle of 16.1° which is well beyond the experiment error. Figure 2(b) plots the simulated diffraction pattern of (14,6) SWNT. Figure 2(c) compares the equatorial intensities of experiment and simulation. These results show an excellent agreement.

The measurement accuracy is critical for large tube structure determination. Figure 3(a) is a pattern from a SWNT of a relatively large diameter. In this case, the diameter and chiral angle were determined to be 3.77 nm (± 0.04 nm) and 20.99° ($\pm 0.2°$), respectively. For large tubes, number of tubes within a range of diameters and chiral angles is much larger than that of small tubes. For example, the possible chiral vectors for Fig. 3(a) are as follows: (34,20) (3.70 nm, 21.49°), (35,20) (3.78 nm, 21.05°), (36,20) (3.85 nm, 20.63°), (36,21) (3.91 nm, 21.36°), (35,19) (3.72 nm, 20.29°), and (35,21) (3.84 nm, 21.79°). When both diameter and angle are considered, (35,20) fits the experimental result the best. Differentiation of these possibilities is only possible with the high measurement accuracy achieved, especially that of chiral angle. Figure 3(b) shows the simulated electron diffraction pattern based on (35, 20). Comparison between Figs. 3(a) and 3(b), however, shows two noticeable differences. First, the absolute distances between the diffraction lines and the equatorial line in the experimental pattern are ~2% larger than those in the simulated pattern. Second, the distances from the diffraction lines especially $(10\bar{1}0)$ and $(01\bar{1}0)$ to the tube axis in Fig. 3(a) are much closer than those of simulation. This discrepancy is due to the tilt of the tube from the plane normal to the electron beam.[15] The distance from a diffraction line to the equatorial line in the case of a tilt of γ, d_γ, is enlarged compared to that for $\gamma=0$, d_0, by a factor of $1/\cos\gamma$. This relationship can be used to calculate γ. For Fig. 3(a), γ was determined to be $13° \pm 1°$. It is also obvious that the tube orientation does not affect the ratio of the distances from diffraction lines to the equatorial line. Thus, the method we proposed to measure the chiral angle is independent of tube orientation.

Single- and multiple- (including double) wall CNTs can be distinguished from the equatorial oscillation without the need of HRTEM imaging. The oscillation comes mostly from interference between scattering off the two sides of the tube, thus, each tube can be approximated by two slits in the Young's interference experiment. Multiple slits from MWNT's introduce an oscillatory envelope to the Bessel oscillation,[13] which, depending on both the number and distances between different walls, can be identified from the intensity profile of the equatorial line.

In conclusion, we present a quantitative technique to measure both the chirality and diameter of the SWNT's from a single electron diffraction pattern. Electron recording with imaging plates is used to improve both the sensitivity and accuracy. The equatorial oscillation was used to determine the diameter of SWNTs and distinguish between different forms of NTs. The chiral angle is measured by using the distances between the diffraction lines to the equatorial line. The accuracy of the measurement of diameter and chiral angle, improved considerably over previous publications, allows an unambiguous determination of the chiral vector (n,m). The validity of this technique is proved by kinematic simulations.

Work on electron microscopy characterization was supported by DOE DEFG02-01ER45923 and DEFG02-91ER45439 and uses the TEM facility of Center for Microanalysis of Materials at FS-MRL. The authors would like to thank R. Tsui and H. Goronkin (Motorola Labs) for supporting this research work.

[1] S. Iijima, Nature (London) **354**, 56 (1991).
[2] C. Dekker, Phys. Today **52**, 22 (1999).
[3] R. Saito, G. Dresselhaus, and M. S. Dresselhaus, *Physical Properties of Carbon Nanotubes* (Imperial College Press, London, 1998).
[4] R. H. Baughman, A. A. Zakhidov, and W. A. de Heer, Science **297**, 787 (2002).
[5] J. W. Mintmire, B. I. Dunlap, and C. T. White, Phys. Rev. Lett. **68**, 631 (1992).
[6] R. Saito, M. Fujita, G. Dresselhaus, and M. S. Dresselhaus, Appl. Phys. Lett. **60**, 2204 (1992).
[7] Z. Yao, C. Dekker, and P. Avouris, Top. Appl. Phys. **80**, 147 (2001).
[8] J. W. Wintmire and C. T. White, Carbon **33**, 893 (1995).
[9] A. Jorio, R. Saito, J. H. Hafner, C. M. Lieber, M. Hunter, T. McClure, G. Dresselhaus, and M. S. Dresselhaus, Phys. Rev. Lett. **86**, 1118 (2001).
[10] S. Iijima and T. Ichihashi, Nature (London) **363**, 603 (1993).
[11] L.-C. Qin, S. Iijima, H. Kataura, Y. Maniwa, S. Suzuki, and Y. Achiba, Chem. Phys. Lett. **268**, 101 (1997).
[12] J. M. Cowley, P. Nikolaev, A. Thess, and R. E. Smalley, Chem. Phys. Lett. **265**, 379 (1997).
[13] M. Kociak, K. Suenaga, K. Hirahara, Y. Saito, T. Nakahira, and S. Iijima, Phys. Rev. Lett. **89**, 155501 (2002).
[14] J.-F. Colomer, L. Henrard, Ph. Lambin, and G. Van Tendeloo, Phys. Rev. B **64**, 125425 (2001).
[15] S. Amelinckx, A. Lucas, and P. Lambin, Rep. Prog. Phys. **62**, 1471 (1999).
[16] J. W. G. Wildoer, L. C. Venema, A. G. Rinzler, R. E. Smalley, and C. Dekker, Nature (London) **391**, 59 (1998).
[17] T. W. Odom, J-L. Huang, P. Kim, and C. M. Lieber, Nature (London) **391**, 62 (1998).
[18] Q. Chen and L.-M. Peng, Phys. Rev. B **65**, 155431 (2002).
[19] A. M. Cassell, J. A. Raymakers, J. Kong, and H. Dai, J. Phys. Chem. B **103**, 6484 (1999).
[20] P. B. Hirsch, A. Howie, R. B. Nicholson, D. W. Pashley, and M. J. Whelan, *Electron Microscopy of Thin Crystals*, 2nd ed. (Krieger, Huntington, NY, 1977), p. 19.
[21] D. Sherwood, *Crystal, X-rays and Proteins* (Wiley, New York, 1976).